# DELIVERABLE REPORT

# FLEXCHX

## Flexible combined production of power, heat and transport fuels from renewable energy sources

| | |
|---|---|
| **Call:** | H2020-LCE-2017-RES-RIA |
| **Topic:** | Developing the next generation technologies of renewable electricity heating/cooling |
| **Grant agreement No:** | 763919 |
| **Start date:** | 01.03.2018  **Duration:** 36 Months |
| **Project Coordinator:** | VTT Technical Research Centre of Finland Ltd |

| | |
|---|---|
| **WP No:** | 2 |
| **Task No:** | 2.3 |
| **Deliverable No**: | 2.1 |
| **Title:** | **Review of electrolysis technologies and their integration alternatives** |
| **Lead beneficiary:** | DLR |
| **Dissemination level:** | Public |

| | |
|---|---|
| **Due date of deliverable:** | Month 6 **/** 2018/08/31 |
| **Actual submission date:** | 2018/08/31 |

## Acceptance

| Name, Company | DD/MM/YYYY |
|---|---|
| Esa Kurkela, VTT | 31/08/2018 |

## History of changes

| Revision | Date | Modification | Author |
|---|---|---|---|
| 1.0 | 13.7.2018 | Original for comments | Sandra Adelung |
| 1.1 | 6.8.2018 | Some comments and questions | Esa Kurkela |
| 2.0 | 30.8.2018 | Final version | Felix Habermeyer |
| 3.0 | 3.9.2018 | Minor corrections | Minna Kurkela, Felix Habermeyer |

## Distribution

| 30/08/2018 | FLEXCXH Share Point and SyGMa |
|---|---|

## Table of acronyms

| AEC | Alkaline Electrolysis Cell |
|---|---|
| AEL | alkaline electrolyzer |
| BtL | Biomass to Liquid process |
| FCH 2 JU | Fuel Cells and Hydrogen Joint Undertaking |
| FT | Fischer-Tropsch |
| PEMEL | proton exchange membrane electrolysis |
| SOEC | solid oxide electrolysis cell |
| TRL | Technology readiness level |

# Table of Contents

# 1 Introduction

Deliverable 2.1 in work package 2 "Concept development" reviews the electrolyzer technologies based on open literature. The main focus is on PEMEL (proton exchange membrane electrolysis) and SOEC (solid oxide electrolysis cell) systems and includes the following studies:

- · Estimated efficiency (suitable for 1-30 MW range)
- · Possibilities for energy integration to improve the efficiency
- · Time spans for start-up, shut-down and load changings
- · Possibilities and costs for storing excess $O_2$

The outcome of this study will be used for work package 8 "Techno-economic and environmental assessment of the process concepts" as well as in designing optimal FLEXCHX process concepts in work package 2.

# 2 Water electrolysis and integration in FLEXCHX

Water electrolysis is a key process in the FLEXCHX process concept, if fluctuating renewable electricity shall be included as a flexible resource. In general, three main electrolysis technologies are available to produce hydrogen from water: AEL (alkaline electrolyzer), PEMEL and SOEC. AEL is the most established technology with relatively low capital costs, but high maintenance costs due to the fact that the electrolyte is highly corrosive and circulation of the electrolyte is required [1]. PEMEL systems provide higher current densities, but have shorter lifetimes and higher investment costs [1]. The SOEC systems are the least developed, but are expected to have improved efficiency especially if the integration of waste heat is possible [1]. Within the FLEXCHX concept the scope is limited to PEMEL and SOEC systems. In 2014 a not legally binding Multi-Annual Work Programme for the second phase of the Fuel Cells and Hydrogen Joint Undertaking (FCH 2 JU) under the EU's Horizon 2020 was published. The key performance indicators (KPIs) for electrolyzer technologies for state-of-the-art (2012) and future targets are shown in Table 2-1. These indicators provide information about predicted efficiency and operation dynamics for water electrolyzers.

*Table 2-1: State-of-the-art and future targets for hydrogen production from renewable electricity for energy storage and grid balancing [2].*

|  |  | 2012 | 2017 | 2020 | 2023 |
|---|---|---|---|---|---|
| KPI 1 | H₂ production electrolysis, energy consumption (kWh/kg) @ rated power | 57-60 @100kg/d | 55 @500kg/d | 52 @1000+kg/d | 50 @1000+kg/d |
| KPI 2 | H₂ production electrolysis, CAPEX @ rated power including ancillary equipment and commissioning | 8.0 M€/(t/d) | 3.7 M€/(t/d) | 2.0 M€/(t/d) | 1.5 M€/(t/d) |
| KPI 3 | H₂ production electrolysis, efficiency degradation @ rated power and considering 8000 h operations / year | 2% - 4% / year | 2% / year | 1.5% / year | <1% / year |
| KPI 4 | H₂ production electrolysis, flexibility with a degradation < 2% year (refer to KPI 3) | 5% - 100% of nominal power | 5% - 150% of nominal power | 0% - 200% of nominal power | 0% - 300% of nominal power |
| KPI 5 | H₂ production electrolysis, hot start from min to max power (refer to KPI 4) | 1 minute | 10 sec | 2 sec | < 1 sec |
| KPI 6 | H₂ production electrolysis, cold start | 5 minutes | 2 minutes | 30 sec | 10 sec |

A further improvement of the efficiency is supposed to be achieved by a detailed energy integration. For example, in this concept the Fischer-Tropsch synthesis is operated at 20-30 bar and the gasification process at 5-10 bar. Hydrogen will be fed into the carbon monoxide rich syngas entering the FT-unit while oxygen is used in the gasification process. Therefore, it might be more efficient to operate the electrolysis at elevated pressure to reduce or even avoid pressurization of the hydrogen. This can be conducted by pressurization of liquid water in PEM or by heating the inlet water above 100 °C in SOEC systems [3]. Heat integration is an issue which will be addressed within the project. This is especially relevant for SOECs because they require high temperature sources.

In the FLEXCHX concept the electrolyzer is operated in the 'summer season' when electricity from solar panels is readily available. In the 'winter season' the process can be run without an electrolysis unit. However, the process can also be used for grid management (diurnal, weekly) by shifting between the two modes ('summer season', 'winter season'). Here, the flexibility of the key components (electrolyzer, gasifier, synthesis unit) defines how efficiently and how quickly the process can shift between the operation modes. Therefore, the flexibility of the electrolyzer unit is one focus in this literature review.

# 3 Proton exchange membrane (PEM) electrolysis

PEM electrolyzers use a proton exchange membrane to separate the protons ($H^+$) from water and oxygen. Operating conditions range between 20-100 °C and up to 100 bar [4]. Schmidt et al. report the operating conditions to be in the range of 50-80°C and >200 bar [5]. A particular concern in PEMEL is the required use of Ir, which is a very rare metal and is considered a critical material (Pt (Pt-Pd) catalyst at the cathode and $RuO_2$ ($IrO_2$) catalyst at the anode [6]). The following reactions take place:

Anode: $$H_2O \rightarrow 0.5\ O_2 + 2\ H^+ + 2\ e^- \tag{1}$$

Cathode: $$2\ H^+ + 2\ e^- \rightarrow H_2 \tag{2}$$
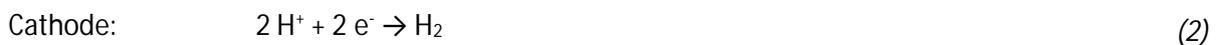
Carmo et al. state that the membrane allows current densities of 0.6-2 $Acm^{-2}$ [6], whereas the more recent study by Babic et al. puts the current density in the range of 1-3 $Acm^{-2}$ [4].

Advantages of the technology are a wide operational range of current densities, excellent dynamic response to variable electricity input and on/off cycling, the possibility to operate at significant differential pressure [4] and the higher $H_2$ purity (99.9% to 99.9999% [7]/ 99.99% [8]) compared to competing systems.

A key feature of the PEM electrolyzer is the system lifetime. Schmidt et al. use expert elections to estimate the development of the lifetime staring from a state-of-the-art system in 2017 [5]. Table 3-1 shows predictions for 2020 and 2030 in contrast to the current system lifetime.

*Table 3-1 Predicted PEMEL system lifetime [5]*

| System Lifetime [h] | 2017 | 2020 | 2030 |
|---|---|---|---|
| Min. | 20,000 | 50,500 | 66,125 |
| Max. | 60,000 | 67,481 | 85,018 |

## 3.1 Efficiency and stack sizes

Bazzanella et al. report the PEM to have reached a technology readiness level of 7-8, which means that the system prototype has been demonstrated in an operational environment and the actual system has been completed and qualified through test and demonstration [9].

Further, they state that first units have been successfully operated for some years, but no full life-cycle has been investigated under operation conditions [9].

One has to distinguish between system, stack and cell level. The system sizes can be increased with additional stacks, whereas a stack is comprised of multiple cells. Thus, the 'scale effect' on the costs is more pronounced when providing larger systems entailing more stacks [10]. Bertucciolo et al. predict the system and stack sizes from 2014 to 2030 (Table 3-2) in consultation with stakeholders [10]. Hereby, the term Central indicates the trend line worked out from the stakeholder consultations. The Range refers to the best and worst case predicted by experts.

*Table 3-2: Predicted system and stack sizes in kW [10].*

| Size | | | 2014 | 2015 | 2020 | 2025 | 2030 |
|------|--------|-----------|------|------|------|------|------|
| kW | System | Central | 180 | 2,100 | 5,400 | 5,900 | 6,400 |
| | | Range [(1)] | 100 - 1,200 | 1,300 - 10,000 | 1,600 - 90,000 | 1,800 - 90,000 | 2,100 - 90,000 |
| | Stack | Central | 50 | 200 | 1,100 | 1,500 | 1,900 |
| | | Range [(1)] | 40 - 100 | 100 - 1,300 | 100 - 10,000 | 500 - 10,000 | 1,000 - 10,000 |

(1) Range for the largest systems offered for use in energy related applications. Smaller systems do exist.

In a study published in 2014, the state of the art was reviewed based on actual offerings (see Table 3-3) [11]. From this data the efficiency for a 5 MW system was estimated to be $\eta_{HHV}$ = 69 % or 1,057 $Nm^3h^{-1}$ $H_2$ at nominal load. For 2030 a 100 MW system was estimated to consist of 10.31 $MW_{el}$ stacks with a corresponding efficiency of $\eta_{HHV}$ = 84 % or 25,311 $Nm^3h^{-1}$ $H_2$ at nominal load. Similarly, Carmo et al. report a voltage efficiency of $\eta_{HHV}$ = 67-82 % [6].

*Table 3-3: State of the art (2014) PEM systems [11].*

| Company | Model series (operating pressure) | $H_2$ rate/ ($Nm^3h^{-1}$) | Status |
|---------|-----------------------------------|---------------------------|--------|
| CETH (FR) | E series (14 bar) | 5 – 60 | Prototype in field test |
| Giner (US) | OGP (207 bar) | 13 | Armaments sector Armaments sector |
| | LPE (55 bar) | ~ 15 | |
| | n.a. (85 bar) | 56 | In development |
| h-tec (DE) | EL 30 (30 bar) | 0.4 – 2.4 | Prototype |
| Areva (FR) | n.a. (30bar) | 1 – 10 | Single-unit for nuclear power plants |
| Hydrogenics (CA) | Hylyzer 65 | Up to 30 | Development rests |
| | HySTAT-P (30 bar) | 250 | Development of prototype |
| ITM Power (GB) | HLab/HPac/HBox (15 bar) | 0.36 – 7 | Pre-series, field test |
| | HFuel (n.a.) | Up to 60 | Prototype in field test |
| | HGas (80 bar) | Up to 60 | Prototype in field test |

| Proton Energy Systems (US) | Hogen GC, S (13.8 bar) | 0.02 – 1.05 | Commercial |
| | Hogen H (15/30 bar) | 2 – 6 | Commercial |
| | Hogen C (30 bar) | 10 – 30 | Prototype, Pre-series in 2010 |
| | HP (165 bar) | | Armaments sector |
| Siemens (DE) | Silyzer 100 (50 bar) | 20 (*) | Prototype in field test |
| | Silyzer 200 (35 bar) (*) | 250 (*) | Development of prototype |
| Sylatech (DE) | n.a. (30 bar) | Up to 0.12 | Single-Unit production |

(*) Data estimated

Wenske proposes the stack efficiency to be in a range of 4.3-9 $kWh(Nm^3)^{-1}$ $H_2$ while he predicted future PEM electrolysis with a specific energy consumption lower than 4.2 $kWh(Nm^3)^{-1}$ $H_2$ [12]. Smolinka et al. state the efficiency as follows: 3.9-5.1 $kWh(Nm^3)^{-1}$ $H_2$ for stacks, 6-8 $kWh(Nm^3)^{-1}$ for systems $<1m^3_N/h$ $H_2$ and $<6$ $kWh(Nm^3)^{-1}$ for systems $>1m^3_N/h$ $H_2$, whereas this study has a major focus on a production rate of 0.1-30 $Nm^3h^{-1}$ $H_2$ [13]. Bertucciolo et al. expect an increase of the system efficiency as depicted in Table 3-4 [10].

*Table 3-4: Expected system efficiency [10].*

| Electricity input [1] | | ~ 2014 | 2015 | 2020 | 2025 | 2030 |
|---|---|---|---|---|---|---|
| $kWh_{el}/kg_{H2}$ | Central | 57 | 52 | 48 | 48 | 47 |
| | Range [2] | 50 - 83 | 47 - 73 | 44 - 61 | 44 - 57 | 44 - 53 |

(1) at system level, incl. power supply, system control, gas drying (purity at least 99.4%). Excl. external compression, external purification and hydrogen storage.
(2) some outliers excluded from range

There are currently no stacks available in the targeted range of up to 30 MW. Although no such stacks are available, it is also possible to operate a 6 MW plant e.g. with 3 x 2 MW stacks - as can be seen in Mainz (SILYZER 200, Siemens) [14]. However, this leads to increasing costs because smaller stacks require comparably more system components. Siemens, Shell and ITM Power are planning the world's largest hydrogen electrolysis plant with a peak capacity of 10 MW (1,300 $tH_2$/year) which is scheduled to be in operation in 2020 at Rhineland refinery, Germany [15]. Further, Siemens is targeting a PEM system with a power input of 100 MW beyond the year 2020. The basis for this system size lays a new product generation Silyzer 300 with 6 MW [16].

Large stacks available exceeding 2 MW input are currently provided by Hydrogenics Corporation and Giner ELX.

Hydrogenic's largest stack is a 3 MW system (HyLYZER 600) with a hydrogen production rate of 620 $Nm^3h^{-1}$ [17]. It is operated at up to 35 bar and has a stack efficiency of $\eta_{HHV} = 75\text{-}80$ % at 3-2 MW, respectively [18]. Hydrogenics 1 MW stack provides 229 $Nm^3h^{-1}$ $H_2$ at nominal load

and 290 $Nm^3h^{-1}$ $H_2$ at a maximum load of 1.5 MW - with a total energy consumption range of 4-5.2 $kWh(Nm^3)^{-1}$ $H_2$ [19].

Giner's largest stack is a 5 MW system (Kennebec) providing 2,200 kg $H_2$/day at up to 15.5 bar [20].

In conclusion, there is currently no PEM system operational with a power input of 15 MW, the planned scale of the FLEXCHX process. However, as stacks in the MW range are already availed by the producers Hydrogenics, Giner and Siemens, it is likely that the hurdle of combing those stacks into an electrolyzer system will be overcome by the year 2025. This assumption is supported by that fact that Siemens is targeting an even larger scale of 100 MW beyond 2020.

## 3.2    Energy integration

Increased temperature leads to less electrical energy requirement. Temperatures above 100 °C can be reached with pressurized systems, maintaining the liquid state of water [4]. However, material stability issues arise with temperatures above 100 °C, which lead to a typical operating range between 60-70 °C for commercial systems [4]. A typical pressure range for commercial electrolyzers is between 30-50 bar. Babic et al. state that if hydrogen and oxygen at a pressurized state are of interest in the downstream process, a balanced pressure PEM system is favorable over differential and ambient pressure, due to the lower efforts for drying and compression [4].

In the FLEXCHX process hydrogen is required at 20-30 bar pressure and the required oxygen pressure in the gasification process is 7-12 bar. However, oxygen storage may require higher pressures as is discussed in Chapter 5 of this report. Waste heat is available at different temperature levels.

It is also advantageous in the context of the FLEXCHX process that the PEM system produces highly pure product streams. The gaseous oxygen and hydrogen streams are separated almost entirely from the liquid water feed in the PEM cell. Schmidt et al. report a hydrogen purity of 99.9 % [5]. Similarly, Albrecht et al. state that the anode output can be assumed to be pure oxygen [21]. Consequently, no additional purification steps have to be included before feeding the products into the FLEXCHX process.

## 3.3    Flexibility

The PEM system responds rapidly to power input fluctuations. In fact, Ursua et al. state that the PEM electrolyzer shows the quickest response to load variations compared to the

alternative systems AEC and SOEC [22]. Similarly, Schmidt et al. quantify that a PEM electrolyzer responds within milliseconds while AEC and SOEC respond within seconds [5].

When looking at dynamic systems the flexibility has to include (Table 3-5):

(i)      a definition of minimum part load operation

as well as time spans for ramping from:

(ii)      start-up time (cold) to minimum part load,
(iii)     minimum part load to full load,
(iv)     full load to minimum part load.

*Table 3-5: Expected flexibility key performance indicators [10].*

| | | | 2014 | 2015 | 2020 | 2025 | 2030 |
|---|---|---|---|---|---|---|---|
| (i) | % (full load) | Central | 9% | 7% | 4% | 4% | 4% |
| | | Range | 5% - 10% | 3% - 8% | 0% - 5% | 0% - 5% | 0% - 5% |
| (ii) | Minutes | Central | 5 | 5 | 5 | 5 | 5 |
| | | Range | 5 - 15 | 5 - 15 | 5 - 15 | 5 - 15 | 5 - 15 |
| (iii) | % (full load) /second | Central | 40% | 40% | 40% | 40% | 40% |
| | | Range | 10% - 100% | 10% - 100% | 10% - 100% | 10% - 100% | 10% - 100% |
| (iv) | % (full load) /second | Central | 40% | 40% | 40% | 40% | 40% |
| | | Range | 10% - 100% | 10% - 100% | 10% - 100% | 10% - 100% | 10% - 100% |

Noack et al. predict the efficiency for

·    a low risk scenario: 5 MW system $\rightarrow$ $\eta_{HHV}$ = 64% at 150 % nominal load for 30 minutes
·    a high risk scenario: 100 MW system $\rightarrow$ $\eta_{HHV}$ = 77 % at 200 % nominal load for 30 minutes for 2030 [11].

For a 50 kW system producing 7.50 $Nm^3h^{-1}$ $H_2$ it took 60 s from maximum operating power to minimum part load operation and 28 minutes from cold standby to maximum operating power [23].

For a 1 MW stack from Hydrogenics response times were found to be as following [19]:

·    from minimum part load to 500 kW (150 kW to 500 kW): 15 s producing 100 $Nm^3h^{-1}$ $H_2$

- from minimum part load to nominal load (150 kW to 1 MW): 30 s producing 200 $Nm^3h^{-1}$ $H_2$
- from minimum part load to maximum load (150 kW to 1 MW): 43 s producing 290 $Nm^3h^{-1}$ $H_2$

Expressing this in terms of Table 3-5 this leads to 2.8 % (full load)/second for ramping to nominal load. Additionally, a stepwise increase with an interval of 150 kW from 250 kW to 1500 kW was performed, leading to system efficiency between $\eta_{HHV}$ = 69-77 %, whereby a maximum efficiency was reached at 400 kW [19]. Start-up time for a cold start takes over 25 minutes for this system [24].

## 3.4   Capital Expense

Presently, the capital costs for a PEMEL system is reported to be in the range of 1860-2320 € $kW^{-1}_{el}$. This price range makes the PEMEL cheaper than the available SOEC systems, yet more expensive than the AEC systems (Alkaline Electrolysis Cell) ranging in between 1000 and 1200 € $kW^{-1}_{el}$ [5]. Schimdt et al. identify platinum catalyst and the fluorinated membrane material as the major cost drivers for a PEMEL [5]. Therefore, current development efforts are targeted at finding less expensive materials. Further, the capital costs for a PEMEL system can be decreased by reducing the complexity of the manufacturing process [5].

A different study published by Andrews and Bahmans assumes a lower price of 1500 $ $kW^{-1}_{el}$. They further estimate the PEMEL cost to drop to 1000€ $kW^{-1}_{el}$ by 2030 [25].

Schmidt et al. also estimate the cost development of the PEMEL by eliciting predictions from fuel cell experts [5]. According to their study, most experts estimate the PEMEL price to drop into the range of 700-1200 € $kW^{-1}_{el}$ in 2020 and into the range of 500-1200 € $kW^{-1}_{el}$ in 2030. This development would level the price for PEMEL and AEL systems – even when factoring in the expected price drop for the AEL.  Contrarily, a minority of the experts expects the PEMEL price to stay above today's AEL price [5].

In a similar study, Saba et al. outline the price development for PEMEL and alkaline electrolyzers. This is accomplished by a comprehensive literature review of papers dealing with price estimations for this technology. In Figure 1 these cost prediction in $€_{2017}$ $kW_{HHV-Output}^{-1}$ are plotted over the period from 1990 to 2030 [26].
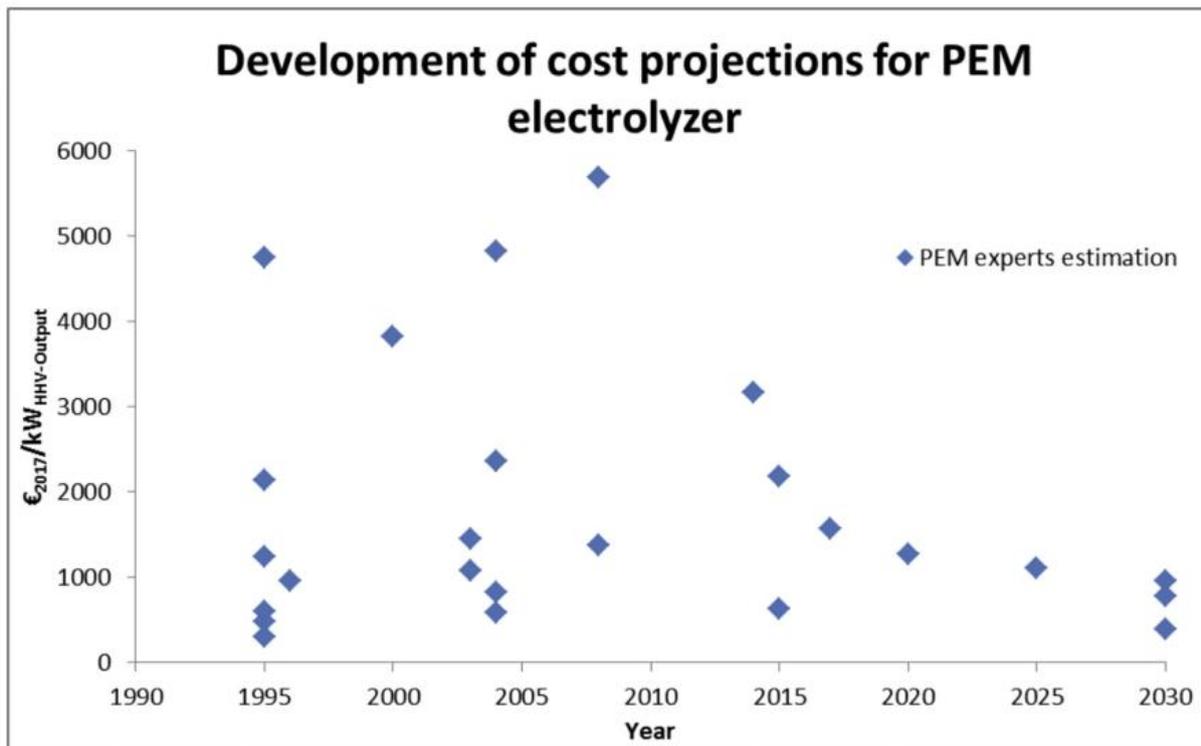
*Figure 1: Development of expected PEM electrolysis cost €/kW$_{HHV-Output}$ based on expert estimations [26]*

For PEM technology, the spread of the estimations in the 1990s was in the range between 306 and 4748 €$_{2017}$/kW$_{HHV-Output}$. Today's estimations for the future investment costs (year 2030) are narrowed towards the values of 397 and 955 €$_{2017}$/kW$_{HHV-Output}$. The findings in Figure 1 imply, similar to the findings of Schmidt et al., that the investment costs for a PEM system will drop below 1000 €$_{2017}$/kW$_{HHV-Output}$ by approximately 2020.

In Figure 2 the price development for alkaline electrolyzers is shown. In addition to expert estimations, Saba et al. include actual manufacturer prices.
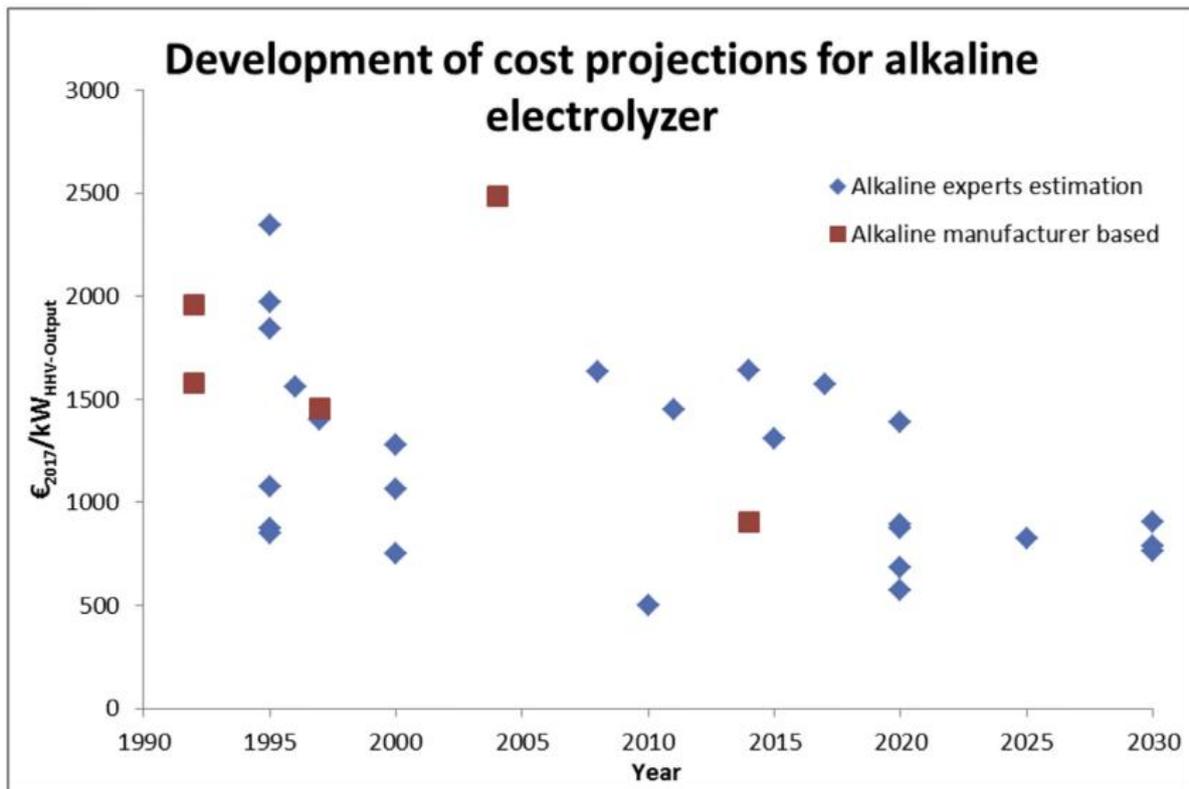
*Figure 2: Development of expected alkaline electrolysis cost €/kW$_{HHV-Output}$ based on expert estimations [26]*

For alkaline technology, the spread of the estimations in the 1990s was in the range between 873 and 2347 €$_{2017}$/kW$_{HHV-Output}$. Today's estimations for the future investment costs (year 2030) are narrowed towards the values of 787 and 906 €$_{2017}$/kW$_{HHV-Output}$. Again, the trend in Figure 2 points towards a price below 1000 €$_{2017}$/kW$_{HHV-Output}$ [26].

In the case of AEC systems, the cost reduction is expected to come from an improved supply chain and a higher production volume. The PEMEL investment costs, on the other hand side, will decrease due to technical developments and better production methods in combination with an economy scale [26].

## 3.4 Conclusions on the potential use of PEMEL in the FLEXCHX process

The literature review indicates that the PEMEL is an interesting technology for the FLEXCHX process. Firstly, it is highly likely that the PEM system size will reach the required 15 MW by the time the FLEXCHX process would enter the market in 2025. Stacks in the MW range are already available from the producers Hydrogenics, Giner and Siemens. The hurdle of combining those stacks in a larger electrolyzer system will probably be overcome because

Siemens is already planning for a 10 MW system in 2020 and a 100 MW system beyond 2020 [16].

The investment costs for a PEMEL are estimated to decrease over the coming years into an area, which is economically sensible for the FLEXCHX process. Starting from investment costs presently around 2000 €/kW the costs are predicted to drop below the 1000 €/kW line by the year 2020. The FLEXCHX project statement assumes investment costs for the electrolyzer of 600 €/kW in 2030 for a 15 kW system and an overall investment volume of 70-75 M€. These requirements could be met if the predicted price drop can be realized [5].

Also the operation costs can be kept at a relatively reasonable level. Firstly, the efficiency of a PEM electrolyzer is in the range of 67-82 % [6]. Secondly, a PEMEL system can be operated for 20,000 – 60,000 h [5]. Thirdly, both products, oxygen and hydrogen, are produced with a high purity. Therefore, no additional purification units are required [22].

A key feature of the FLEXCHX process is the switching between two modes of operation. This can only by accommodated by a flexibly operated electrolysis system. The 28 min needed for a cold start shown for a PEM system found by Lettenmaier et al. [19] is sufficient – especially when compared to the predicted flexibility of the gasification and Fischer-Tropsch units in FLEXCHX.

# 4  Solid oxide electrolysis cell (SOEC)

In SOEC systems steam is fed to the cathode, where the conversion to $H_2$ and $O^{2-}$ takes place. Oxygen ions are transported through the electrolyte consisting of Yttria stabilized Zirconia (YSZ) [5] to the anode side where they react to molecular oxygen. The utilized catalyst is Ni/YSZ at the cathode and Perovskite-type lanthanum strontium manganese (La0.8Sr0.2MnO3) stabilized on YSZ at the anode [5]. In comparison to PEM systems further processing of the product gases is required because it consists of a mixture of hydrogen and steam [1]. The charge carrier is $O^{2-}$, a ceramic membrane works as electrolyte and typical current densities vary between 0.5-1 $Acm^{-2}$. Other sources [27] [28] report a larger attainable current density range of 0.3-2 $Acm^{-2}$. The reactions taking place are as follows:

Cathode:  $H_2O + 2\,e^- \rightarrow H_2 + O^{2-}$  (3)

Anode:  $O^{2-} \rightarrow 0.5\,O_2 + 2\,e^-$  (4)

Typical operating conditions vary between 700-1,000 °C. The high temperature operation decreases the electricity demand (cell voltage), but also leads to an increasing heat demand with temperature [1]. In endothermic mode even an electrical efficiency above 100 % can be achieved in theory (increased heat demand) [1]. This is of special interest where an integration of high temperature waste heat is available and can be integrated with economic benefits [1].

In contrast to PEM and alkaline electrolyzers, which can only convert $H_2O$ to $H_2$, the SOEC is also able to operate with a $CO_2$ feed or even a mixture of $H_2O$ and $CO_2$ gas. The latter process is referred to as co-electrolysis [29]. In case a $CO_2$ feed is present the cathode reaction is stated as [30]:

Cathode: $\qquad CO_2 + 2\,e^- \rightarrow CO + O^{2-}$ (5)

Jensen et al. investigated the co-electrolysis at 750 °C under different operating pressures of 0.4-10 bar and found that the pressure only has a weak effect on the performance [3]. Contrarily, Lehner et al. report an upper pressure boundary at 25 bar [8]. Ebbesen found that optimizing the cell pressure for a given current densities can yield a lower cell voltage [31].

A key feature of the SOEC electrolyzer is the system lifetime. Schmidt et al. use expert elections to estimate the development of the lifetime staring from a state-of-the-art system in 2017 [5]. Table 4-1 shows predictions for 2020 and 2030 in contrast to the current system lifetime.

*Table 4-1 Predicted system lifetime for an SOEC [5]*

| System Lifetime [h] | 2017 | 2020 | 2030 |
|---|---|---|---|
| Min. | <10,000 | 39,500 | 80,000 |
| Max. | - | 50,924 | 102,222 |

## 4.1   Efficiency and stack sizes

In principle, high-temperature electrolyzers can attain a higher efficiency than low-temperature electrolyzers. This is due to the fact that the dissociation reaction of water requires less electrical energy. The reaction's enthalpy change ΔH can be expressed by the sum of Gibb's free energy change ΔG and the heat supplied to the system Q, which is equivalent to the temperature T of the system times the corresponding entropy change ΔS [22].

$$\Delta H = \Delta G + Q = \Delta G + T\Delta S \qquad (6)$$

According to Ursua the energy for this endothermic reaction is provided as thermal energy (T∆S) and electrical energy equivalent to the free Gibb's energy (∆G) [22]. Figure 3 shows how the energy demand changes with the operation temperature of the electrolysis. It is apparent that the electrical energy demand is reduced while the thermal energy demand is increased with the rising operation temperature.
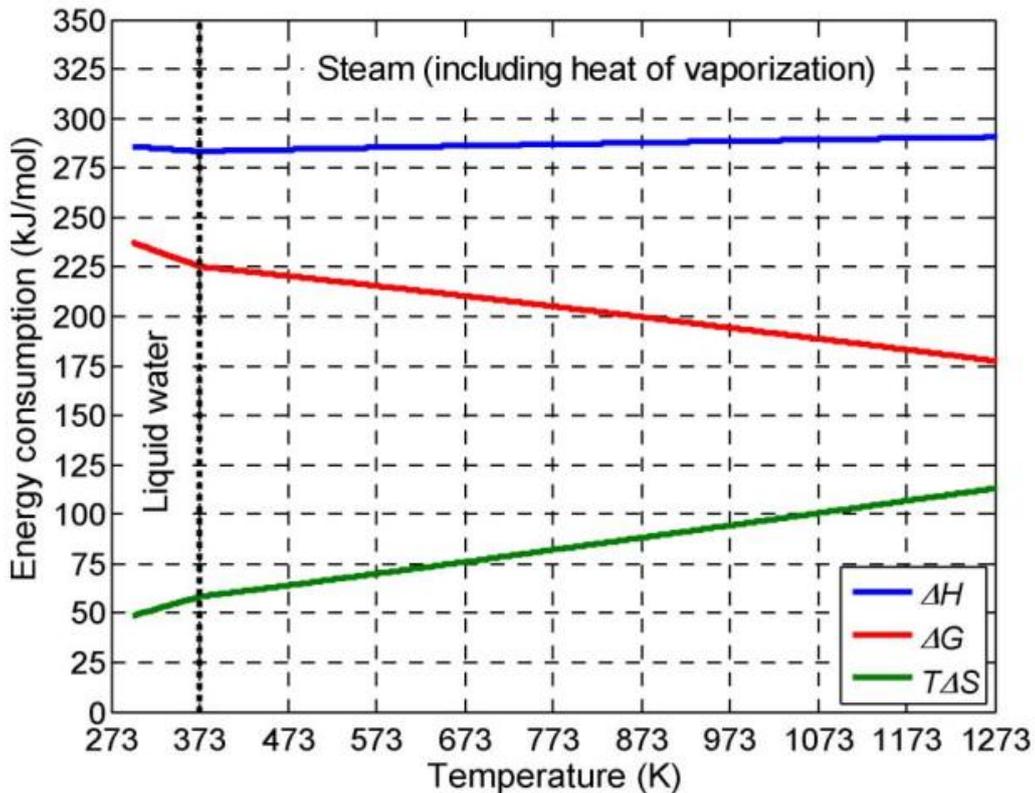


*Figure 3 Evolution of the energy consumption of an ideal electrolysis at 1 atm [22]*

The overall efficiency of an electrolyzer can be defined by the ratio of the electrical power input and the lower/higher heating value (LHV/HHV) of the produced hydrogen stream ($\dot{V}_{H2}$) [13].

$$\eta_{LHV} = \frac{\dot{V}_{H2} \cdot LHV}{P_{el}} \qquad (7)$$

$$\eta_{HHV} = \frac{\dot{V}_{H2} \cdot HHV}{P_{el}} \qquad (8)$$

Consequently, high-temperature electrolyzers with their lower electrical energy demand can reach a higher efficiency. Additionally, Graves states that high-temperature cells nearly always have a lower internal resistance than low-temperature cells [32].

In line with these theoretical findings, Schmidt et al. find the high-temperature system SOEC to have a higher efficiency than the low-temperature PEMEL [5]. Table 4-2 shows the electrical energy required to produce a norm cubic meter of hydrogen for a state-of-the-art PEMEL and SOEC stack. It can be concluded that with a high-temperature SOEC up to 70% more hydrogen can be produced with the same energy input [5].

*Table 4-2 Comparison of efficiency for high- and low-temperature electrolyzers [5]*

|  | PEMEL | SOEC |
| --- | --- | --- |
| Operating Temperature [°C] | 50-80 | 650-1000 |
| Stack energy [$kWh_{el}/m_{H2}^3$] | 4.2 - 5.5 | >3.2 |

Bazzanella et al. (2017) found the SOEC to have reached a technology readiness level (TRL) of 6-7, which means that the system/subsystem model or prototype has been demonstrated in a relevant or an operational environment [9]. They expect further progress to lift the TRL to 9 by 2030.

In a 2011 study (planSOEC) Richter et al. state the electrical system consumption at beginning of life as follows [33]:

- State of the Art:      $3.3 \text{ kWh}_{el}(\text{Nm})^{-3} \text{ H}_2$ (heat for steam generation)

       $3.7 \text{ kWh}_{el}(\text{Nm})^{-3} \text{ H}_2$ (electrical steam generation)
- Theoretical potential: $3.2 \text{ kWh}_{el}(\text{Nm})^{-3} \text{ H}_2$ (heat for steam generation)

       $3.6 \text{ kWh}_{el}(\text{Nm})^{-3} \text{ H}_2$ (electrical steam generation)

In 2016, sunfire delivered an SOEC electrolyzer to Boeing with a nominal capacity of 140 kW, which can be operated in fuel cell and electrolysis mode. The system produces 42 $m^3h^{-1}$ $H_2$ with up to 85 % efficiency [34].

In June 2017, sunfire delivered a steam electrolysis module to Salzgitter Flachstahl GmbH with a nominal input power of 150 $kW_{AC}$ and a production rate of 40 $Nm^3h^{-1}$ $H_2$ and an AC system efficiency of $\eta_{LHV,el}$ = 84 % [35].

Further, sunfire is planning a 20 $MW_{AC}$ SOEC system comprised of SynLink modules for the industrial park of Heroya, Norway in 2019. The aim of this project is to incorporate a co-electrolysis system into a power to liquid process producing 8 kt per year. Sunfire claims that the SynLink SOEC has an efficiency of $\eta_{LHV,el} > 80$ % [36]. Operating an SOEC at this scale would prove the feasibility for the FLEXCHX project where an SOEC of up to 30 MW is required.

Lehner et al. report a voltage efficiency of $\eta_{HHV,} = <110$ % for an SOEC with a production rate of <40 $Nm^3h^{-1}$ $H_2$ [8].

## 4.2 Energy integration

Heat integration is a major subject in SOEC systems because electrical energy can be replaced by less exergetically valuable thermal energy [37].

Heat integration in an SOEC plant consists of different recuperators using hot product streams and external heating (Figure 4). External heating is required partially for preheating and for vaporizing the water feed. In a high temperature heat exchanger further heat is required to reach the inlet temperature of 700-900 °C, which can be supplied by an electric heater or an external heating source. In addition to that, heat sources with very high temperatures can be directly integrated in the SOEC stack via the anode side by a heated oxygen sweep stream (endothermal operation) in order to decrease the electrical energy demand. [37]

Buttler et al. investigated the heat integration in SOEC systems and found the following: In thermo-neutral operation the electrical energy consumption varies below 1 % (3.05-3.07 kWh$(Nm^3)^{-1}$) at a temperature range of 700-900 °C. If the SOEC is not operated thermo-neutrally, only a slight decrease in specific electrical energy demand can be reached (3.037 kWh$(Nm^3)^{-1}$) (adiabatic case). With further external heat integration and in isothermal mode (limit case) the specific electrical heat demand can be decreased down to 2.7-2.75 kWh$(Nm^3)^{-1}$ (maximum total heat demand). However, this leads to a significant increase in specific cell area in comparison to thermo-neutral operation. [37]

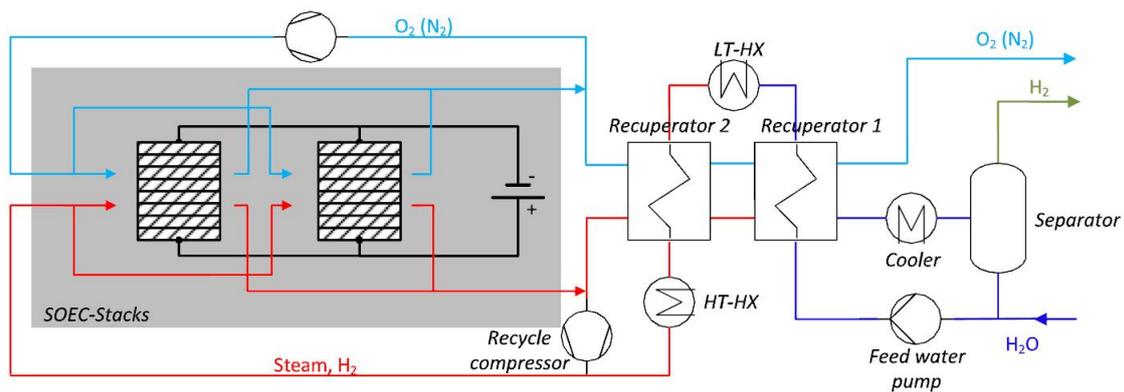Bazzanella et al. state a possible reduction of the electricity demand down to 2.6 kWh$(Nm^3)^{-1}$ [9].

*Figure 4: Simplified scheme of an HTE plant [37].*

Concerning the costs Buttler et al. found: Heat integration decreases the specific electrical energy consumption and current densities but also the hydrogen production, which leads to increasing investment costs. However, lifetime is increasing with lower current densities, which decreases the investment costs. They found heat integration economically reasonable compared to thermo-neutral operation, especially with increasing electricity prices and stack lifetimes. However, in cases of low capacity utilization application (high fluctuations) heat integration tends to be unreasonable because lower operational costs do not outweigh significantly higher investment costs. [37]

Clausen compares conventional wet biomass drying system for biofuel production (Figure 5 right) to a novel process approach (Figure 5 left). As depicted in Figure 5 on the left, the novel approach uses a steam dryer that provides the feed steam for the SOEC. In the conventional approach the steam is produced in a boiler. Clausen reports that producing the steam for the SOEC enables the novel process to handle 82-84 % more water content than the conventional process [38].
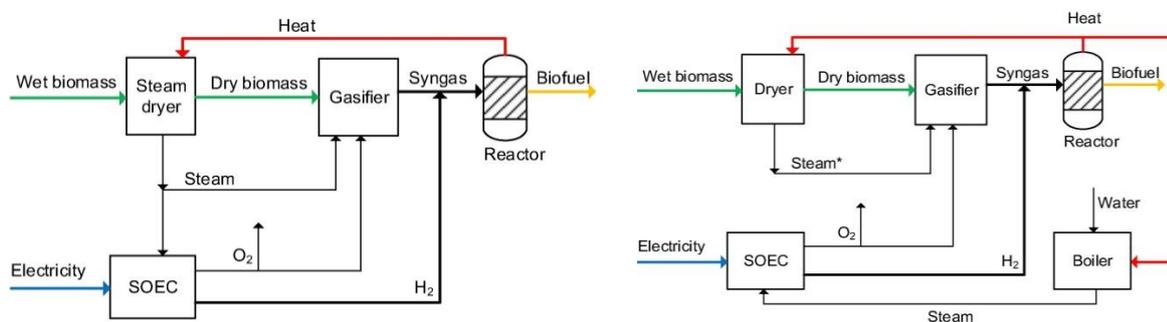


*Figure 5: Left: System for utilization of very wet biomass and electricity for biofuel production; right: "conventional" system for integration of steam electrolysis and biomass gasification for biofuel production. *only if a steam dryer is used. [38]*

Cinti et al. report an increase in the overall efficiency of 10.8 % when introducing a light-gas recycle to Fischer-Tropsch synthesis coupled with an SOEC performing co-electrolysis. For

the base case (A) operated without a recycle the study states an overall efficiency of 46.4 %. In a first process variation (B) Cinti et al. introduce a recycle with an external steam reformer fed by FT light gas. Thereby, the efficiency can be raised to 56.0%. With a direct injection of the light-gas into the SOEC system (internal reforming) in the next variation (C) the overall process efficiency reaches 57.2 % [39].

Herz et al. [29] compare the results of Cinti et al. [39], König et al. [40] and Becker et al. [41] all dealing with combinations of an SOEC and a FT-synthesis featuring a recycle. Based on their processes with the respective overall efficiency of 57.2 %, 44.6 % and 51 %, Herz et al. develop a process with an efficiency of 68 % [29]. Further, Herz et al. categorize three different ways in which the FT by-product gas stream can be utilized. As depicted in Figure 6, option a) reintroduces the FT tail gas into the dry syngas stream. This route, referred to as the short recycle, increases the overall conversion of syngas. Alternatively, the tail gas can be introduced in the $CO_2$ feed for the syngas production, as shown in the route b). This long recycle enables the conversion of by-products back into syngas. Lastly, in route c) the tail gas is combusted to provide heat for the SOEC. The combination of routes c) and b) leads to the high efficiency of 68 % [29].
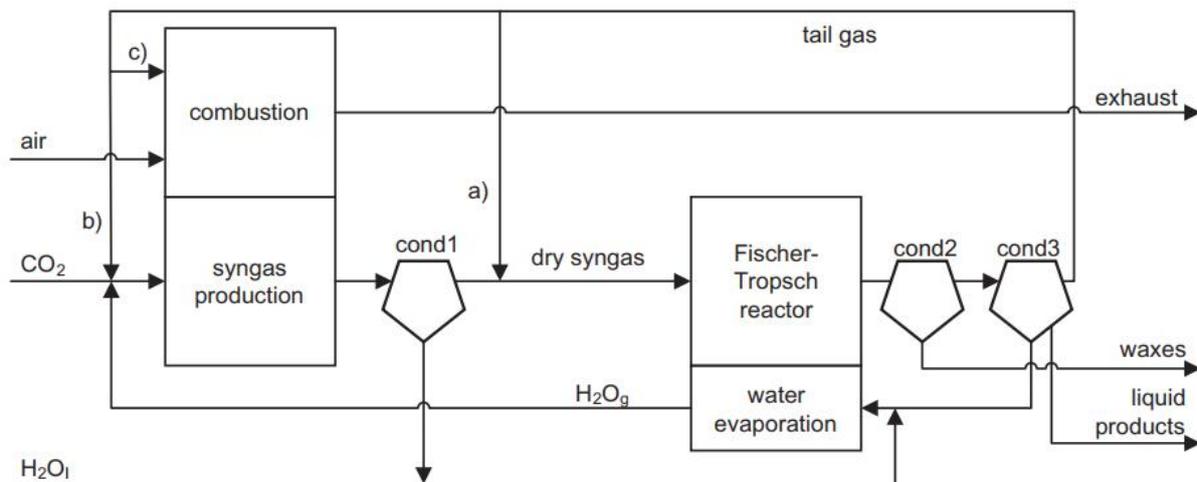


*Figure 6 Simplified process scheme showing three ways of gas utilization: a) short recycle b) long recycle and c) tail gas combustion [29]*

An SOEC co-electrolysis recycle can also be used in the context of a biomass to liquid process BtL. Pozzo et al. show that by including the SOEC recycle in a DME process a plant efficiency of 69.5 % can be reached. In addition, a specific productivity of 0.86 $kg_{DME}/kg_{Biomass}$ is attainable with the recycle [42]. Contrary to the proposed FLEXCHX process design, the $CO_2$ produced in the gasifier is directly introduced into the SOEC cathode.

When integrating the SOEC into the FLEXCHX process the system has a disadvantage concerning the purity of the produced hydrogen stream. The product stream leaving the cathode side is a mixture of steam and hydrogen [22]. However, for the following FLEXCHX process pure hydrogen is needed. The further processing step of splitting this mixture results in additional investment and operation costs for the SOEC. A corresponding separator is also included in the flowsheets of Herz et al. and Bazzanella et al. as seen in Figure 4 and Figure 6.

## 4.3 Flexibility

Smolinka et al. state that load changings lead to temperature changes in the stacks, which reduces the lifetime of the SOEC stacks due to micro cracks in the ceramic. Although the SOEC, in principle, is capable of very fast electric load changings, this lifetime reduction limits the dynamic operation potential. Start-up and shut-down procedures have to be conducted slowly and the temperature should be kept above 600 °C. From this point of view the SOEC seems less appropriate for following fluctuating regenerative power sources [13].

Mathiesen et al. expect a cold start-up time to be in the range of several hours [43]. Garzon-Real et al. also report a start-up time of several hours for the SOEC in contrast to only minutes for a PEMEL. The longer start up time of the SOEC presents a disadvantage in the context of the dynamic FLEXCHX process [44].

The 150 kW – solid oxide cell from Sunfire in Salzgitter is able to operate in overload and is therefore able to reach up to 50 Nm³/h hydrogen output at a power input of approximately 200 $kW_{AC}$. This setup was operated in endothermic mode at 50 % load, which decreased the system efficiency to $\eta_{LHV,el}$ = 75 % (the balance of plant power input has to be increased to prevent the system from cooling down) [35]. The sunfire SynLink SOEC operated at 20 MW is described to have a dynamic range of 30-100% of its nominal load. In addition, sunfire states that this model has a rapid response time and is able to handle any $CO_2/H_2O$ load of the feed gas [36].

In the project Green Industrial Hydrogen (GrInHy) Schwarze et al. found that load can be decreased and increased with gradients up to 10 $kW_{AC}min^{-1}$. The dynamic range is between 50-125 % of nominal operation. However, no information about the degradation is given within the publication. Another objective of this project is to prove a system lifetime over 7,000 hours and stack lifetimes exceeding 10,000 hours with a degradation lower than 1%/1,000 hours. [35]

## 4.4 Capital Expense

The current SOEC price of >2000 € $kW^{-1}_{el}$ is significantly higher than the prices for the competing systems AEC and PEMEC. However, the SOEC is the most recently developed technology with a corresponding high potential for price reduction. The main challenge lies in the material degradation that is due to the high operation temperature in the cell. Thus, finding a more stable material or decreasing the operating temperature would increase the cell's lifetime, thereby bringing down its capital costs [5]. Schmidt et al. report a stack lifetime for an SOEC of <10,000 hours, which is low compared to the 20,000 – 60,000 hours for a PEMEL [5].

According to the expert estimation for the SOEC capital costs conducted by Schmidt et al., the best case prediction ranges between 1300-3000 € $kW^{-1}_{el}$ for the year 2020. In the longer timeframe until 2030, many experts see the costs dropping to the level of 500-1000€ $kW^{-1}_{el}$ making the SOEC a competitive option to the mentioned alternatives [5].

## 4.5 Conclusions on the potential use of an SOEC in the FLEXCHX process

The literature review indicates that the SOEC technology is a promising alternative to PEM systems in the future. However, at the current state-of-the-art using an SOEC appears not to be sensible.

On the one hand, the SOEC technology has great potential. The SynLink electrolyzer by sunfire, which will be installed in Norway by 2019, is set out to be the first SOEC operated with 20 MW [36]. Therefore, the scale planned for the FLEXCHX process seems feasible. Additionally, the SOEC system offers the possibility for heat integration because it is operated at a higher temperature than all other electrolyzer systems [5]. The higher operating temperature also enables a higher efficiency compared to the other electrolyzer technologies because the a) the electrical energy needed to split the feed molecules is lower and b) the high temperature cells have a lower internal resistance than low temperature cells [32].

However, the current technology readiness level does not qualify the SOEC for the FLEXCHX process, as only systems on the kW scale are available at the moment. Further, the capital costs for an SOEC system exceed the costs for the alternatives PEMEC and AEC [5] [26].

Nevertheless, the SOEC is estimated to have the largest improvement potential in terms of technical and economical parameters [5] [26]. This could make the SOEC a viable option for the FLEXCHX process in the future. Especially since, the SOEC opens the possibility for more intensive heat integration. As the SOEC is on the trajectory to become an interesting process

alternative, the simulation should feature a case that captures the development potential for this system.

# 5  Oxygen storage

In general, oxygen can be stored in pressure vessels, in cryo-tanks or in caverns. Those technologies are linked with different technical challenges and different cost structures. In order to match the techno-economical properties with the requirements of the FLEXCHX process, a comprehensive analysis of all possible storage options is performed in the following.

The seasonal storage in the FLEXCHX process requires high capacities and a long residence time. Therefore, the storage technology should feature low investment costs per volume as well as low diffusion loss to the environment [45].

## 5.1  Underground storage

Underground storage of gases can be divided into porous media and cavern storage. In porous media storage the gas occupies the naturally occurring pore space (mineral grains, crystals in sandstones or porous carbonates) which can be found in depleted oil/gas fields or aquifers. In caverns the gas is contained by dense rock or salt, whereby salt caverns are the most common types of man-made storage vessels. Underground natural gas storage facilities are usually operated at 70-170 bar. [46]
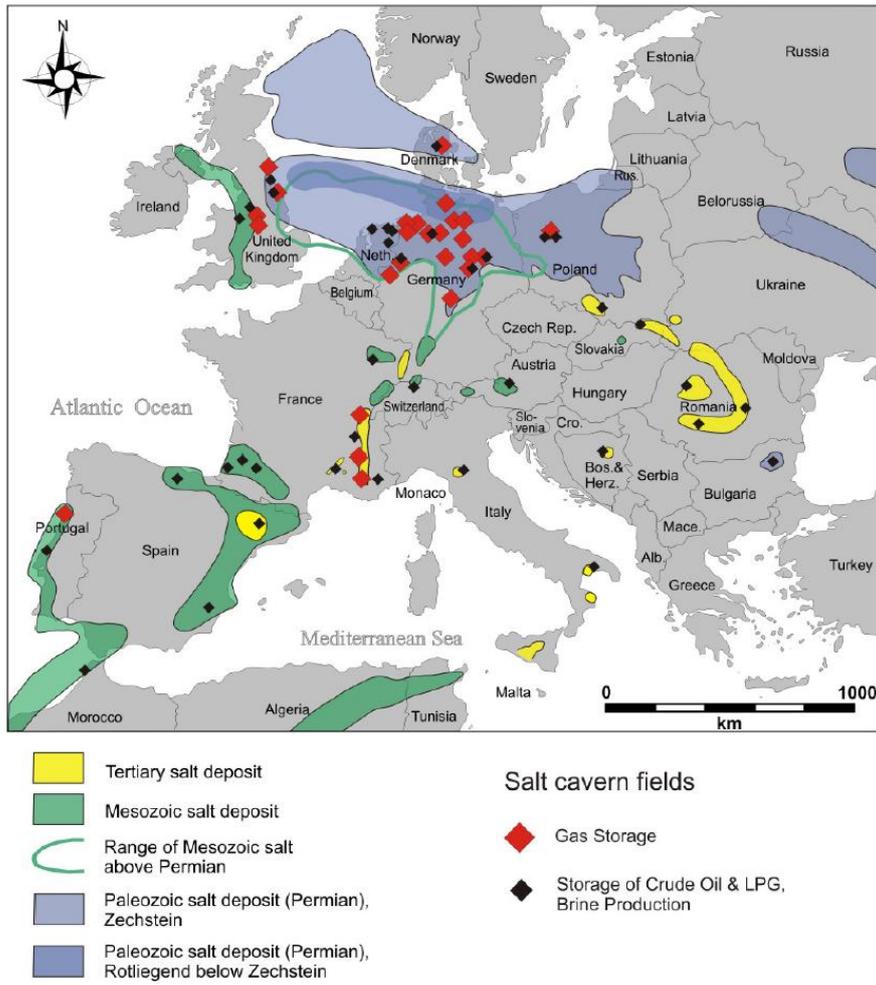
*Figure 7: Salt cavern potentials in Europe [47]*

*Figure 8: Worldwide salt cavern potentials [48]*

Typical salt cavern sizes range from 200,000-800,000 m$^3$ [49].

Figure 7 and Figure 8 show the salt resources on a European and a worldwide scale. As the FLEXCHX project focuses on northern Europe, or more specifically Finland and Lithuania, it becomes obvious that salt caverns are not available in this area.

In comparison to salt caverns another possibility, as discussed in terms of compressed air storage (CAES), are natural aquifers. Regarding that option specific tests have to be conducted in order to determine reactions between the oxygen and the rocks or microorganisms, which might lead to oxygen depletion or blockage of the pores. When considering depleted natural gas fields the issue of possible mixing of residual hydrocarbons with the air arises. Caverns for compressed air storage are operated at approx. 70 bar [50].

Hans-Georg Fasold states that investment and operational cost for porous media and cavern storage are in the same order of magnitude, whereby major cost differences may arise due to different geological and physical conditions [51].

## 5.2    Storage in vessels

In general, one advantage of gas storage in vessels compared to underground storage is the flexibility in terms of geological and physical conditions of the site. The oxygen can be stored either as liquid or high pressure gas, whereby liquefaction is energy intensive, but leads to lower storage capacities due to the higher volumetric density. Typical storage tanks for liquid

oxygen range from 500 to 420,000 gallons (1,893 – 1,589,873 Liters), which leads to maximum storage capacity of approximately 1.4 million $m^3_N$ per tank [52].

Agbossou et al. use a pressure vessel in a PEMFC system to store the excess oxygen produced via electrolysis. In this 5 kW fuel cell system oxygen is stored at 8 bar in a 1 $m^3$ pressure vessel. In this paper the cost of pressurizing the oxygen is described as a significant contribution to the operation costs. The energy effort $E_{comp}$ for the compression can be calculated using following equation [53]:

$$E_{comp} = \frac{p_0 V_0}{(k-1)\eta} \left\{ 1 - \left( \frac{p_{out}}{p_{in}} \right)^{(k-1)/k} \right\}$$ (9)

According to Agbossou et al., the polytropic constant $k$ is equal to 1.4 for diatomic gases. Taking into account the inlet and outlet pressure $p_{in,out}$ as well as the compressor efficiency $\eta$, the compression energy demand can be obtained. Hereby, this energy demand should only be attributed to the storage process if the subsequent step requires a lower pressure level. Ideally, the next process step would be operated at the storage pressure [53].

Increasing pressure and thereby decreasing storage volume leads to lower investment costs. However, the increased pressure demands more pressure resistant materials for the storage vessel. Thus, an optimal storage pressure has to be found for every process keeping the investment cost small while finding a suitable pressure for the subsequent process step.

A different storage approach is discussed in Braun et al., where oxygen is pumped into the cryo-vessel in the liquid state. When stored at 115 bar and -175°C the liquid oxygen has a density of 1128 kg/$m^3$ [54]. Thus, the vessel volume is significantly lower compared to a pressure vessel. However, the gas liquefaction requires additional energy. A second disadvantage of cryo-vessels is the gas loss to the environment due to diffusion. In their study of an electrolyzer coupled with a fuel cell by oxygen and hydrogen storage, Darras et al. assume a loss of 0.01 % of the maximum volume per month for $H_2$ as well as $O_2$ [55]. A different source reports a higher loss rate in the range of 1 - 2% per day for $H_2$ [56]. However, they refer to small size vessels. The loss inversely correlates with the storage volume. Therefore, this source states that large-scale storage tanks can be operated up to 200 days with hardly any losses.

In principle, oxygen can also be stored by adsorbing the molecule at an oxygen-selective material. One possible material was found by Sundberg et al., where crystalline salts of a series of cationic multimetallic cobalt complexes were used in a chemisorption process, that reversibly bind $O_2$ [57]. Although adsorption/chemisorption work in principle, no industrial scale

storage unit is based on this technology, yet. In contrast, the same principle is applied for hydrogen storage e.g. in metal hydrides [58].

## 5.3  Estimation of investment costs via hydrogen analogy

In lack of reliable sources specifically dealing with the oxygen storage investment costs, the costs will be approximated with those for hydrogen storage technologies. Reuß et al. use the following equation in combination with the assumptions in Table 5-1 to calculate the investment costs for various hydrogen storage options [45]. In this approach the investment costs $Invest_{Base}$ for a storage unit with the size $Invest_{Compare}$ are multiplied with the required size $Capacity$ to obtain the corresponding investment costs $Invest_{Total}$. Scale effects can be taken into account via the exponent $Invest_{Scale}$ [45].

$$Invest_{Total} = Invest_{Base} \left( \frac{Capacity}{Invest_{Compare}} \right)^{Invest_{Scale}} \tag{10}$$

*Table 5-1: Economic data for different $H_2$ storage technologies [45]*

|  | Cavern | Tank (GH2) | Tank (LH2) | Liquefaction |
|---|---|---|---|---|
| $Invest_{Base}$ | 81 M€ | 500 € | 25 € | 105 M€ |
| $Invest_{Compare}$ | 500,000 m$^3$ | 1 kg | 1 kg | 50 t day$^{-1}$ |
| $Invest_{Scale}$ | 0.28 | 1 | 1 | 0.66 |

The cost estimation data in Table 5-1 is stated in relation to the stored mass in the case of a gas tank GH2 and a liquid storage tank LH2. For a cavern, on the other hand, the investment costs scale with the corresponding volume. The investment costs of a liquefaction unit necessary for a liquid hydrogen tank are dependent on the mass throughput per day.

Accordingly, Figure 9 shows the investment costs of different storage alternatives over their gas capacity in tons for oxygen on the upper and hydrogen on the lower scale. The investment costs are calculated using the approach used by Reuß et al. [45] and refer only to hydrogen storage. The oxygen scale is calculated using the molar masses and can only serve as an approximation of the oxygen investment costs. The investment costs for gaseous or liquid tanks scale linearly with the stored mass. The liquefaction unit required for the LH$_2$ vessel shows exponential behavior. Similarly, the investment costs for cavern storage rises asymptotically with the gas mass.

Following from Figure 9, pressure tanks have the lowest investment costs for small gas quantities. Liquid storage vessels are the cheapest alternative for an intermediate capacity followed by caverns which are most inexpensive in the upper ranges. However, this finding relies on the assumption that the liquefaction unit has a throughput equal to 5% of the maximum LH2 tank volume.
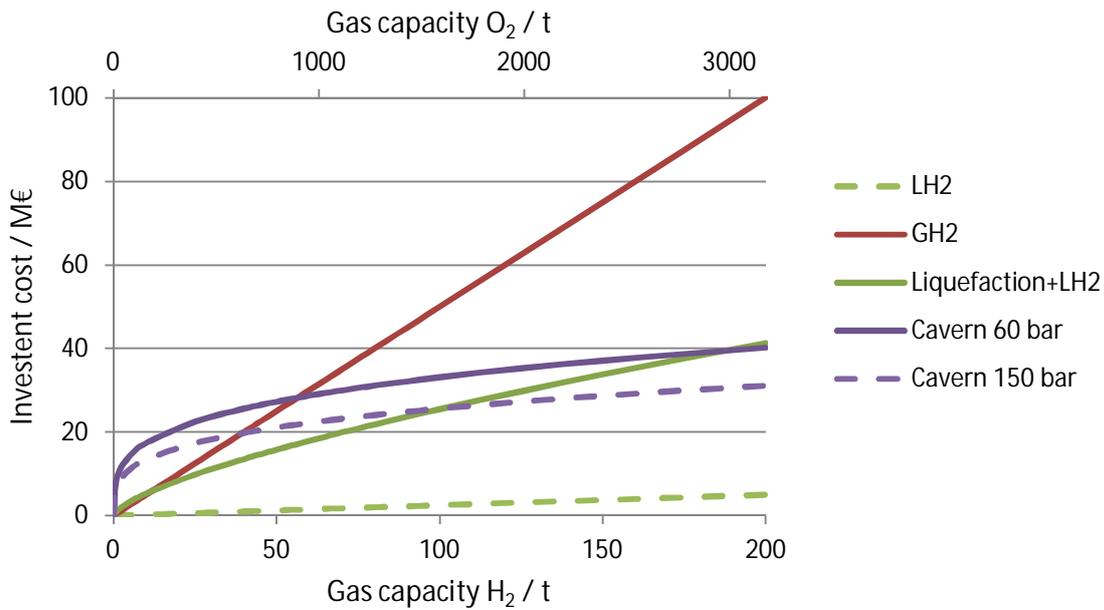


*Figure 9 Estimated investment costs for different hydrogen storage technologies over the gas capacity [45]*

Although the authors could not find a concrete correlation estimating the investment costs specifically for oxygen, some studies touch on the topic of oxygen storage. Doty et al. estimate the capital expenditures for oxygen storage in tanks and liquefaction for 1000 tons of LOX to be 5 $M [59]. Clausen et al. report specific storage cost for hydrogen of 96 €/MWh$_{H2}$. Here, the examined cavern has a storage capacity of 28,000 MWh$_{H2}$ or 840,000 kg$_{H2}$ at a price of 2.7 M€. Clausen at al. also apply this price for oxygen cavern storage. Accordingly, the specific investment costs for oxygen cavern storage amounts to approximately 0.2 €/kg$_{O2}$ at 1,300 t$_{O2}$ [60].

# 6 Conclusion

In this study PEM and SOEC electrolyzers are compared and assessed for their possible use in the FLEXCHX process. In addition, different oxygen storage technologies are evaluated regarding their compatibility to the process and the previously mentioned electrolyzers. Table 6-1 gives a comparative overview of the different electrolyzer technologies.

The PEM electrolyzer seems to be the better suited option within this process framework. Firstly, the PEM features presently the lower investment costs. This difference might cancel out by 2030, as different studies show. But in 2025 the PEM investment costs are probably still lower than those of the SOEC. Secondly, the costs for operating a PEM are smaller compared to the SOEC. This is due to the longer lifetime of the stack. Additionally, the higher purity of the produced hydrogen gets rid of the need for additional purification units. Thirdly, the PEM has better dynamic characteristics than the SOEC. On the one hand, the PEMEL can perform a cold-start within minutes as compared to hours for the SOEC. On the other hand the PEM reacts to load fluctuation within milliseconds and without substantial degradation of the cell.

The SOEC, on the other hand, should not be discarded for this project. The solid oxide electrolyzer, as the most recently developed technology in this field, has the potential for large improvements regarding its technical and economical hurdles. Hence, the comparison with the PEM system might look different by the year 2030. But even today, the technology has some advantages: The high-temperature SOEC has a higher electrical efficiency than the PEM system and it provides the opportunity for more extensive heat integration.

The liquid storage seems to be the most sensible storage option in terms of investment costs. As the FLEXCHX process requires the storage of 3 kt of oxygen, liquid and cavern storage appear to be viable options. However, the FLEXCHX concept is based on the distributed small-scale production units. Yet, cavern storage is only feasible in a limited number of regions in Europe. Therefore, liquid storage has an advantage over all other alternatives. However, the operation costs for storing the oxygen will have to be compared in order to finally choose a storage technology.

At a further stage, in work package 8, the performance of PEM and SOEC electrolysis and alternative oxygen storage methods will be studied in selected FLEXCHX design cases. This deliverable lays the basis for these design cases. For the electrolyzer analysis it is sensible to include cases that predict future technological and economic developments. This is not necessary for the storage technologies, as these are mature technologies. However, since the

information on the capital costs are not reliably documented in the literature other means of getting cost data should be pursued.

*Table 6-1 Comparison of the key aspects relating to PEM and SOEC electrolyzers*

| | | PEMEL | | SOEC |
|---|---|---|---|---|
| Investment cost | + | ~2000 €/kW$_{el}$ (today) → < 1000 €/kW$_{el}$ (2020) [26] [5] | - | > 2000 €/kW$_{el}$ (today) → < 1000 €/kW$_{el}$ (2030) [5] |
| Lifetime | + | 20,000 – 60,000 hours [5] | - | 10,000 hours [5] |
| Product purity | + | Pure hydrogen & oxygen [5] | - | Pure oxygen, hydrogen mixed with steam [21] [5] |
| Start-up time | + | Minutes [5] [44] | - | Hours [5] [44] |
| Dynamic response | + | Milliseconds [5] | - | Seconds [5], detrimental to lifetime [22] |
| Process integration | - | Low potential heat integration | + | Potential for heat integration [29], co-electrolysis [30] |
| Efficiency | - | Low [22] | + | High [22] |
| Scalability | (+) | 100 MW system beyond 2020 planned [16] | (+) | First 20 MW plant in 2019 [36] |

# 7 Bibliography

[1] M. Götz, J. Lefebvre, F. Mörs, A. M. Koch, F. Graf, S. Bajohr, R. Reimert and T. Kolb, "Renewable Power-to-Gas: A technological and economic review," *Renewable Energy*, vol. 85, pp. 1371-1390, 2016.

[2] Fuel cells and hydrogen joint undertaking, *Multi-Annual Work Plan 2014-2020*, 2014, p. 31.

[3] S. H. Jensen, X. Sun, S. D. Ebbesen, R. Knibbe and M. Mogensen, "Hydrogen and synthetic fuel production using pressurized solid oxide electrolysis cells," *International Journal of Hydrogen Energy*, vol. 35, no. 18, pp. 9544-9549, 2010.

[4] U. Babic, M. Suermann, F. N. Büchi and L. Gubler, "Review - Identifying Critical Gaps for Polymer Electrolyte Water," *Journal of The Electrochemical Society*, 2017.

[5] O. Schmidt, A. Gambhir, I. Staffell, A. Hawkes, J. Nelson and S.Few, "Future cost and performace of water electrolysis: An expert elicitation study," *Hydrogen Energy*, 11 2017.

[6] M. Carmo, D. Fritz, J. Mergel and D. Stolten, "A comprehensiv review on PEM water electrolysis," *Hydrogen Energy*, 2013.

[7] F. A. Alexis Michael Bazzanella, "Low carbon energy and feedstock for the European chemical industry," DECHEMA, Frankfurt am Main, 2017.

[8] M. Lehner, R. Tichler, H. Steinmüller and M. Kopper, Power-to-Gas: technology and business models, Springer Briefs in Energy, 2014.

[9] A. M. Bazzanella and F. Ausfelder, "Low carbon energy and feedstock for the European chemical industry," DECHEMA, Frankfurt am Main, 2017.

[10] L. Bertuccioli, A. Chan, D. Hart, F. Lehner, B. Madden and E. Standen, "Development of Water Electrolysis in the European Union," Fuel Cells and Hydrogen Joint Undertaking, 2014.

[11] DLR, LBST, Fraunhofer ISE, KBB, "Studie über die Planung einer Demonstrationsanlage zur Wasserstoff-Kraftstoffgewinnung durch Elektrolyse mit Zwischenspeicherung in Salzkavernen unter Druck," Bundesministerium für Wirtschaft und Energie, 2015.

[12] M. Wenske, "Wasserstoff - Herstellung per Elektrolyse," Stralsund, 2008.

[13] T. Smolinka, M. Günther and J. Garche, "Stand und Entwicklungspotenzial der Wasserelektrolyse zur Herstellung von Wasserstoff aus regenerativen Energien," Nationale Organisation Wasserstoff- und Brennstoffzellentechnologie, 2011.

[14] Siemens, "Energiepark Mainz - Weltweit größte PEM-Elektrolyseanlage 2015".

[15] Shell, ITM Power, FCH, *EUROPEAN CONSORTIUM WITH SHELL AND ITM POWER ANNOUNCE AGREEMENT TO BUILD ELECTROLYSIS AT RHINELAND REFINERY,* 2018.

[16] Hydrogeit, "HZwei-Blog," 9 8 2017. [Online]. Available: https://www.hzwei.info/blog/2017/08/09/viel-los-bei-gp-joule-thyssenkrupp-siemens/. [Accessed 23 8 2018].

[17] Hydrogenics, "Hydrogenics Unveils 3 Megawatt PEM Electrolyzer Stack," 25 04 2017. [Online]. Available: http://www.hydrogenics.com/2017/04/25/hydrogenics-unveils-3-megawatt-pem-electrolyzer-stack/. [Accessed 05 2018].

[18] Hydrogenics, "Hydrogenics' HyLYZER® 600: Enabling a utility scale renewable hydrogen solution, with the smallest footprint," 2017.

[19] P. Lettenmeier, T. Smolinka, B. Pitschak, A. Bayer and R. Schoof, "Abschlussbericht: Kompaktes 1 MW-PEM-Wasserelektrolyse-System - Regenerativer Wasserstoff für Mobilität und Energiespeicherung," Uniper Energy Storage GmbH, Essen, 2016.

[20] U. Küter and M. Bromeis, "PEM-Elektrolyse-Stacks für Systemintegratoren," 10 03 2016.

[21] F. Albrecht, D. König, N. Baucks and R.-U. Dietrich, "A standardized methodology for the techno-economic evaluation of alternative fuels – A case study," *Fuel,* 2017.

[22] A. Ursua, L. Gandia and P. Sanchis, "Hydrogen Production From Water Electrolysis: Current Status and Future Trends," *Proceedings of the IEEE,* 2012.

[23] W. Waiblinger, P. Lettenmeier, R. Reißner, M. K. A. S. Gago, T. Kathrotia, J. Grohmann, P. Oßwald, W. Meier and U. Riedel, "Abschlussvortrag: Future Fuels TP2 - Chemische Energiespeicher," DLR, Stuttgart, 2018.

[24] S. You, C. Træholt, P. Marcuello, R. Reissner and Y. Zong, "Deliverable Report: Standardized qualifying tests of electrolysers for grid services," FCH JU2, 2017.

[25] J. Andrews and B. Shabani, "Dimensionless analysis of the global techno-economic feasibility of solar-hydrogen systems for constant year-round power supply," *Hydrogen Energy,* 2011.

[26] S. Saba, M. Müller, M. Robinius and D. Stolten, "The investment costs of electrolysis - A comparison of cost studies from the past 30 years," *Hydrogen Energy,* 2017.

[27] M. Laguna-Bercero, "Recent advances in high temperature electrolysis using solid oxide fuel cells: a review," *Journal of Power Sources,* 2012.

[28] H. Steinmüller, G. Reiter, R. Tichler, C. Friedl, M. Furtlehner and J. Lindorfer, Power to Gas - eine Systemanalyse. Markt- und Technologiescouting und -analyse, Im Auftrag des BMWFJ, 2014.

[29] G. Herz, E. Reichelt and M. Jahn, "Techno-economic analysis of a co-electrolysis-based synthesis process for the production of hydrocarbons," *Applied Energy,* 2018.

[30] C. Graves, S. Ebbesen, M. Mogensen and L. Klaus, "Sustainable hydrocarbon fuels by recycling CO2 and H2O with renewable or nuclear energy," *Renewable and Sustainable Energy Reviews,* 2010.

[31] S. D. Ebbesen, "Solid Oxide Electrolysis Cells - High pressure operation," in *International Symposium on Water Electrolysis and Hydrogen as part of the future Renewable Energy System*, Copenhagen, 2013.

[32] C. Graves, Recycling CO2 into Sustainable Hydrocarbon Fuels: Electrolysis of CO2 and H2O, Columbia University, 2010.

[33] A. Richter, C. F. Pedersen, M. Mogensen, S. H. Jensen, M. Sloth, M. Chen and J. U. Nielsen, "planSOEC - R&D and commercialization roadmap for SOEC electrolysis R&D of SOEC stacks with improved durability," ???, 2011.

[34] Sunfire, "Sunfire supplies Boeing with world's largest commercial reversible electrolysis (RSOC) system," Dresden/USA, 2016.

[35] K. Schwarze, O. Posdziech, S. Kroop, N. Lapeña-Rey and J. Mermelstein, "Green Industrial Hydrogen via Reversible High-Temperature Electrolysis," ECS Transactions, 2017.

[36] sunfire GmbH, 2018. [Online]. Available: https://www.sunfire.de/de/produkte-und-technologie/sunfire-synlink. [Accessed 16 August 2018].

[37] A. Buttler, R. Koltun, R. Wolf and H. Spliethoff, "A detailed techno-economic analysis of heat integration in high temperature electrolysis for efficient hydrogen production," *International Journal of Hydrogen Energy,* vol. 40, no. 1, pp. 38-50, 2015.

[38] L. R. Clausen, "Energy efficient thermochemical conversion of very wet biomass to biofuels by integration of steam drying, steam electrolysis and gasification," *Energy,* no. 125, pp. 327-336, 2017.

[39] G. Cinti, A. Baldinelli, A. Di Michele and U. Desideri, "Integration of Solid Oxide Electrolyzer and Fischer-Tropsch:," *Applied Energy,* 2016.

[40] D. König, M. Freiberg, R.-U. Dietrich and A. Wörner, "Techno-economic study of the storage of fluctuating renewable energy in liquid hydrocarbons," *Fuel,* 2015.

[41] W. Becker, R. Braun, M. Penev and M. Melaina, "Production of FischereTropsch liquid fuels from high temperature solid oxide co-electrolysis units," *Energy,* 2012.

[42] M. Pozzo, A. Lanzini and M. Santarelli, "Enhanced biomass-to-liquid (BTL) conversion process through high temperature co-electrolysis in a solid oxide electrolysis cell (SOEC)," *Fuel,* 2014.

[43] B. V. Mathiesen, I. Ridjan, D. Connolly, M. P. Nielsen, P. Vang Hendriksen, M. Bjerg Mogensen, S. Højgaard Jensen and S. Dalgaard Ebbesen, "Technology data for high temperature solid oxide electrolyser cells, alkali and PEM electrolysers," Department of Development and Planning, Aalborg University, 2013.

[44] J. Garzon-Real, S. Kilicsoy, B. Dahlmann, T. Kornrumpf, M. Stötzel and M. Zdrallek, "Coupling electricity and gas distribution networks: applications and further steps in the concept development," in *International ETG Congress*, Bonn, 2017.

[45] M. Reuß, T. Grube, M. Robinius, P. Preuster, P. Wasserscheid and D. Stolten, "Seasonal storage and alternative carriers: A flexible hydrogen supply chain model," *Applied Energy,* no. 200, pp. 290-302, 2017.

[46] N. Ferrari, L. Mancuso and P. Cotone, "Operating flexibility of power plants with CCS," International Energy Agency, 2012.

[47] A. Gillhaus, "Natural Gas Storage in Salt Caverns - Present Status, Developments and Future Trends in Europe," Basel, 2007.

[48] G. Gill and G. Cowan, *Adavale Basin, Queensland Underground Salt Cavern Potential.*

[49] K. Görner and D. Lindenberger, "Technologiecharakterisierungen in Form von Steckbriefen," Ministerium für Innovation, Wissenschaft und Forschung des Landes Nordrhein-Westfalen, 2015.

[50] Energy Storage Association, "www.energystorage.org," [Online]. Available: http://energystorage.org/compressed-air-energy-storage-caes. [Accessed 05 2018].

[51] H.-G. Fasold, "Untertägige Speicherung von Erdgas - Speicherbedarf für Europa und die Schweiz:Strukturierung, Kosten, Potenziale," 2010.

[52] Air Products, "Liquid oxygen".

[53] K. Agbossou, M. Kolhe, J. Hamelin, E. Bernier and T. K. Bose, "Electroytic hydrogen based renewable energy system with oxygen recovery and re-utilization," *Renewable Energy,* 2003.

[54] R. Braun and K. Kattke, "Evlauating SOFC-based Power System Concepts for Unmanned Undersea Vehicles," in *ECS Transactions*, 2009.

[55] C. Darras, S. Sailler, C. Thibault, M. Muselli, P. Poggi, J. Hoguet, S. Melscoet, E. Pinton, F. Gailly, C. Turpin, S. Astier and G. Fontes, "Sizin of photovoltaic system coupled with hydrogen/oxygen storgae based on the ORIENTE model," *International Journal of Hydrogen Energy*, 2010.

[56] "energieportal24," [Online]. Available: http://www.energieportal24.de/cms1/wissensportale/brenn-kraftstoffe/wasserstoff/h2-speicherung/. [Accessed 26 6 2018].

[57] J. Sundberg, L. Cameron, P. Southon, C. Kepert and C. McKenzie, "Oxygen chemisorption/desorption in a reversible single-crystal-to-single-crystal transformation," *Chemical Science*, 2014.

[58] B. Sakintuna, F. Lamari-Darkrim and M. Hirscher, "Metal hydride materials for solid hydrogen storage: A review," *Hydrogen Energy*, 2007.

[59] F. D. Doty, G. N. Doty, J. P. Staab and a. L. L. Holte, "TOWARD EFFICIENT REDUCTION OF CO2 TO CO FOR RENEWABLE FUELS," Phoenix, USA, 2010.

[60] L. Clausen, N. Houbak and B. Elmegaard, "Technoeconomic analysis of a methanol plant based on gasification of biomass and electrolysis of water," *Energy*, 2010.

[61] R. Otten, "The first industrial PtG plant - Audi e-gas as driver for the energy turnaround," CEDEC Gas Day 2014, Verona, 2014.

[62] K. Atsonios and K. Panopoulos, "Investigation of technical and economic aspects formethanol production through CO2 hydrogenation," *Hydrogen Energy*, 2016.

[63] Q. Fu, C. Mabilat, M. Zahid, A. Brisse and L. Gautier, "Syngas production via high-temperature steam/CO2 co-electrolysis: an economic assessment," *Energy & Environmental science*, 2010.